

# Quadrupole Electromagnetic Linear Positioning System (QELPS): Optimal Design, Modelling and Analysis for Linear Motion Application

**Kintali Manohar<sup>1</sup>, Kondamudi Srichandan<sup>2</sup>**

<sup>1</sup>Research Scholar, Department of Electrical, Electronics and Communication Engineering,  
GITAM School of Technology, GITAM deemed to be University,  
Visakhapatnam, India.  
email:mkintali@gitam.edu

<sup>2</sup>Assistant Professor, Department of Electrical, Electronics and Communication Engineering,  
GITAM School of Technology, GITAM deemed to be University,  
Visakhapatnam, India.  
e-mail: skondamu@gitam.edu

**Abstract**—In linear motion systems, including linear motors and actuators, precise and controlled linear motion is provided for various applications. However, they have several drawbacks: high costs, complexity, limited stroke length, high energy consumption, speed limitations, heat generation, noise and vibration, limited load capacity, environmental considerations, and integration challenges. High costs are especially significant for applications requiring high precision. The components' complexity and additional control electronics can increase maintenance and trouble-shooting requirements. Ensuring accurate and efficient operation necessitates regular maintenance. The limitation in stroke length, determined by the drive's size and guide length, can pose challenges for applications requiring long strokes. High energy consumption can be a concern, and speed limitations may be challenging. Managing heat generation is crucial to prevent component damage. Noise and vibration can be problematic, particularly in quiet applications. Integration challenges can arise when dealing with complex systems or automation processes. To overcome some of these drawbacks, an innovative coil configuration design for linear positioning system applications is proposed. The proposed design focuses on the Quadrupole Electromagnetic linear Positioning System (QELPS), comprising four coils generating a uniform electromagnetic field to produce a Lorentz force on the slider. The QELPS design is meticulously crafted using 3D modeling in ANSYS software, and the magnetic characteristics indicate the potential for scaling this model to different levels. The power circuit of the QELPS is simulated using ANSYS Simplorer and incorporates silicon-controlled rectifiers (SCR) and a pulse width modulation (PWM) pulse generator. The design achieves a force of 27.6 newtons with the paper presenting current and force plots in comprehensive detail. Furthermore, an interactive design algorithm is introduced, facilitating the customization of this model for various linear track dimensions. This research aims to advance linear drive technology and enhance linear motion applications by developing this new coil configuration design and harnessing the Quadrupole Electromagnetic System

**Keywords**- Linear motion; QELPS; Electromagnetics; FEM; ANSYS 3D simulations; Interactive computing.

## I. INTRODUCTION

Automation industries are inducing positional linear motion drives for robotic operations such as conveyers, sliders, and workbench operations. For better control and accuracy in the process, linear electrical motors are under supervision. For positional linear motion to advance, several essential research needs have emerged, each offering promising opportunities for innovation and improvement.

Linear drives work on two principles, i.e., rotational motion to linear motion and direct generation of linear motion. A linear motor converts electric energy into linear motion. Compared to other comparable technologies, linear motors offer several advantages; some are less friction, easy operation, wide speed

range, etc.[1]. A few famous linear motors, such as linear induction motors, linear synchronous motors, and linear reluctance motors, are under use by some industries. Linear motors can produce several megawatts of mechanical power at speeds ranging from 200 to 550 km/h for applications such as High-Speed Public Transportation Systems (MAGLEV) and Urban Metros [2]. Ongoing projects such as the German Trans Rapid, the Japanese JR-MLX, the Japanese HSST, and the Canadian Bombardier Metro are significant 21st-century challenges [3]. Even in high-performance machine tools, direct linear drives show their application. High-precision positioning axes are possible by combining high-force linear motors, high-resolution position sensors, and cutting-edge current and position loop controllers.

Linear drives can provide high forces of up to 10,000 N, speeds of up to 10 m/s, and acceleration of up to 25 g. Traditional rotary drive motors and ball screws create table motion in CNC machine tools. In [4], a low-cost, high-speed cutting machine utilizes linear motors to perform machining experiments on a composite material. The device has standard CNC router capability and can reach table speeds of over 40 m/min and spindle speeds of 30,000 rev/min.

Direct drives with linear motors have recently piqued the interest of both business and research. The lack of mechanical reduction and transmission mechanisms in these systems increases the effect of various unknown electromechanical phenomena [5] (e.g., friction, cogging forces, etc.) and load disturbances considerably more substantial than in traditional rotary actuators. Ironless linear motors can achieve high dynamics, speed stability, and precision. When mounted on air-bearing systems, they can provide exact trajectories with an inaccuracy of less than 20 nm [6]. Linear Drives can provide high dynamic movements with minor stroke linear stages. Moving coils provide dynamic solid force but only modest continuous force. Moving magnets provide greater forces with less activity [7]. Their forces range from 1 to 700 N, and their strokes can reach 75 mm. Direct linear drives have opened the doors for novel designs and configurations of the coils in the system. This paper proposes a new coil configuration for linear positioning system applications. A Quadrupole Electromagnetic Linear Positioning System (QELPS) is a linear drive consisting of four coils that provide a uniform electromagnetic field to generate a Lorentz force on the slider.

[8] proposed a Multipole Electromagnetic device. According to the research, this model has good force and velocity characteristics. [9] examined the MFEL model for double-sided armature. The coaxial positioning of the coil within and outside the armature improves the flux density in the system. The same researcher examined a tiny inner armature weighing 63.13 g and a massive outside armature weighing 88.38 g. Multi-stage twisted multipole electromagnetic launching [10,11,12] is a concept for countering the magnetic pull due to rotational motion. According to this paradigm, while the armature accelerates, the armature spins by its axis. For vehicles, the authors propose an evacuated tube launch mechanism. These research needs underscore the multidisciplinary nature of positional linear motion drives, encompassing materials science, control theory, tribology, and sustainability. Addressing these challenges will pave the way for more efficient, precise, and sustainable linear motion systems, driving advancements in numerous industries.

Electromagnetic systems are also known for precision and versatility in linear positioning systems. Some of the electromagnetic systems used as linear positioning systems are linear induction motors (LIM), Linear synchronous motors (LSM), Electromagnetic solenoid actuators, and voice coil

actuators (VCA). These linear positioning systems are used in various industries like manufacturing, robotics, transportation, and aerospace varied research is going on to refine these systems as they have certain disadvantages. According to the research, the multipole field launching principle is fascinating and relevant. Various MFEL analyses, such as the use of flux distribution [13, 14, 15,16,17], coil twisting [18, 19, 20], other armature shapes research [21, 16], and optimal design [22] utilizing different methods, are also helpful in learning more about the MFEL. Different switching patterns are explained out of which best switching pattern is found to obtain maximum Lorentz force in this article [23]. [24] proposes a Two-wing Ring type Armature, which can accommodate any type of material inside the ring working on an electromagnetic induction principle for propelling the object.

The utilization of Multipole Electromagnetics in linear positioning systems represents an innovative strategy for achieving precise and efficient motion control [25]. This technique involves the strategic placement of multiple magnetic poles along the linear path, generating intricate magnetic field patterns. These patterns find applications across various domains, including linear positioning systems. In contrast, conventional linear positioning systems often rely on straightforward magnetic setups, such as solenoids or permanent magnets, which, while effective, can exhibit limitations concerning precision and adaptability. Multipole Electromagnetics [26, 27, 28], conversely, exploits the concept of strategically positioned multiple magnetic poles to create meticulously controlled magnetic fields. These fields can be precisely manipulated to achieve exceptionally accurate linear motion by adjusting the strength and polarity of individual poles. For example, in a linear motor employing Multipole Electromagnetics, the stator comprises an array of magnetic poles, each independently controllable. Coordinating the energizing and de-energizing of these poles enables the linear element (such as a carriage or slider) to move with remarkable precision and fluidity. This heightened level of control proves invaluable in applications demanding the utmost precision, such as semiconductor manufacturing, optics positioning, or laboratory automation.

This article introduces the concept of a Quadrupole Electromagnetic Linear Positioning System (QELPS), inspired by the Multipole Electromagnetic Launcher. The QELPS is a non-contact sensor that can measure the position and velocity of a moving object with high accuracy. The article presents a detailed description of the design algorithm for the QELPS, which includes the selection of the magnetic material, the calculation of the magnetic field strength, and the determination of the optimal sensor position. The modeling of the QELPS is also discussed, including the use of finite element analysis (FEA) to simulate the magnetic field and the use of ANSYS to analyse the data. The mathematical model explains the workings

of the model. QELPS model can be applied for any motion track positioning system with square rod support.

The article provides a thorough explanation of the theory behind the QELPS, including the principles of magnetic fields and the quadrupole configuration. The use of QELPS in manufacturing industries can have several benefits, such as enabling precise control of the position of objects along the manufacturing process and detecting deviations from the intended path. This can help to improve the quality of products and reduce waste. The design algorithm and modeling approach in the proposed QELPS model of the article provide valuable insights into applications in various motion track positioning systems featuring solid bar support.

## II. DESIGN STRUCTURE OF QELPS

Quadrupole Electromagnetic Linear Positioning System (QELPS) consists of sliding bar, yoke, and coils. The idea of this work is to move the coil-filled yoke on a sliding bar based on Faraday's laws of Electromagnetic induction. The sliding bar is the stationary component and the coil-filled yoke is the moving component. In Figure 1 (a), the 3D model of the QELPS is mentioned. The coils are placed on four sides of the sliding bar to apply each Lorentz force. This Lorentz force helps in moving the coil-filled yoke on the sliding bar. The dimensions considered for this study are as mentioned. Each copper coil has 1000 turns with 40mm\*40mm\*68mm dimensions. A yoke made of iron measures 153 mm\*22 mm \* 20mm. The bar also made of iron measures 500 mm\*120 mm\* 60 mm. The dimensions of each component are pictorially represented in Figure 1(b), Figure 1(c), and Figure 1(d).

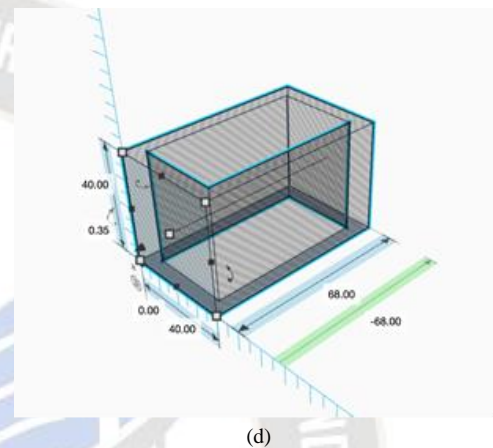
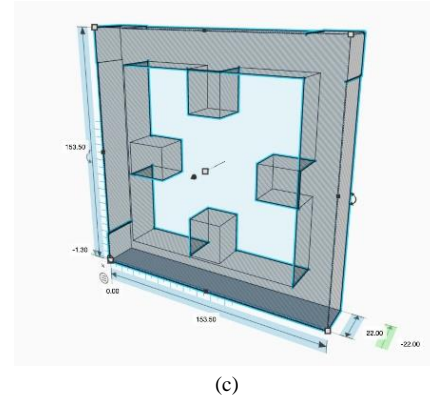


Figure 1. Quadrupole Electromagnetic Linear Positioning System (a) Quadrupole Electromagnetic System, (b) Bar, (c) Rectangular yoke, (d)Coil

The properties of iron considered for this study are conductivity of 103\*105 siemens/m, relative conductivity of 4000, and Poisson's ratio is 0.28. To observe the magnetic characteristics of the QELPS, magnetostatic analysis is conducted using ANSYS Maxwell. For the analysis, 1000 A of current excitation is considered. Figure 2 and 3 explores the magnetic flux density in terms of magnitude and vectors.

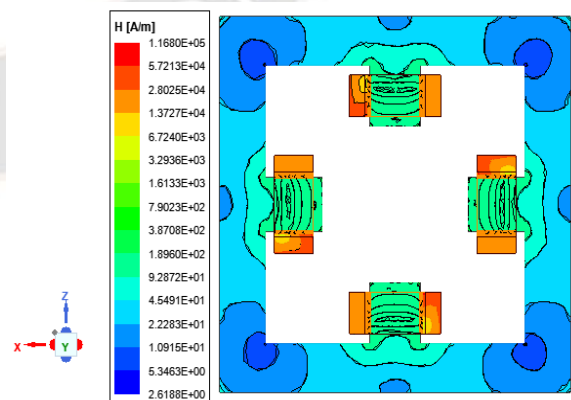
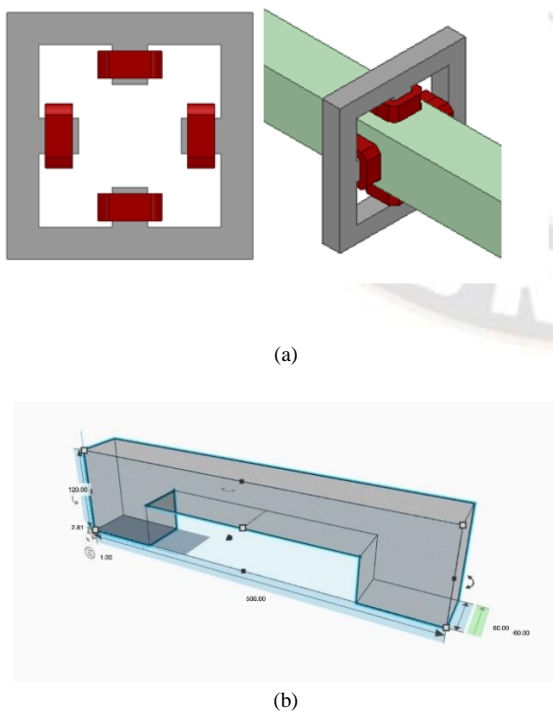


Figure 2. Magnetic Intensity Magnitude in QELPS yoke and coil.

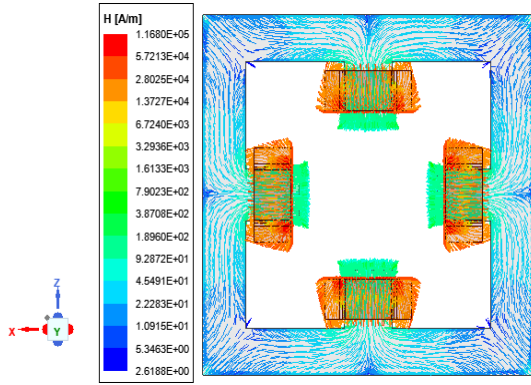


Figure 3. Magnetic Intensity Vectors in QELPS Yoke and Coil

The maximum intensity observed in coils, and the yoke helps close the system's magnetic path.  $1.168 \times 10^5$  A/m is the maximum intensity, and 2.61 A/m is the minimum intensity. The magnetic density of 3.58 Tesla is the maximum, and 0.0038 Tesla is the minimum. In the yoke, the magnetic field is uniform and points inward, providing consistent and tightly packed field vector lines. In the coil, the magnetic intensity's vector is determined by the electric current passing through it. The vector direction is circular, and its magnitude depends on the current strength. More current means a stronger magnetic field with a larger vector.

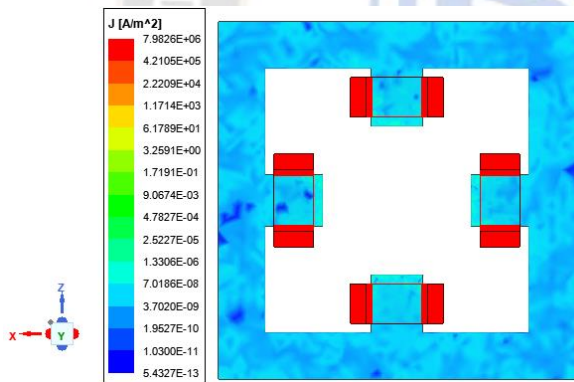


Figure 4. Current density in the yoke and coils of QELPS

Current density is a plot that will help understand the system's hotspots. In Fig. 4, the current density of the system is presented. The current density is maximum in the coils, which implies that the coils will be hotspots, and the yoke is a bit cooler than the coils.

The circuit modeling and the motion expression of the core, yoke, and coils are given in Equations. 1-5 (Kim et al., 1996)

$$\{[L_i] + [M_i]\} \frac{d}{dt} [I_i] = [V_i] - [R_i][I_i] - v_p [G_i][I_i] \quad (1)$$

$$[c_i] \frac{d}{dt} [V_{ci}] = -[I_{di}] \quad (2)$$

$$r_o \frac{dv_p}{dt} = \frac{1}{2} [I_i]^T [G_i][I_i] \quad (3)$$

$$\frac{dx}{dt} = v_p \quad (4)$$

$$[G_i] = \frac{d}{dx} [M_i] \quad (5)$$

Where in the above Equations 1-5, suffix i varies from 1 to the number of stages,  $[V_i], [I_i], [V_{ci}]$ , and  $[I_{di}]$  are the voltage and current matrices of the coils and the center bar.  $[C_i], [L_i]$ , and  $[M_i]$  are the capacitance of the capacitor bank with a Source of 30V and self-inductances and mutual inductances of driving coils and center bar.  $r_o$  and  $v_p$  are the mass and velocity of the center bar. Lorentz force observed in the system is 79.651 N in the y-direction.

TABLE I. SELF AND MUTUAL-INDUCTANCE MATRIX

Coils	Coil 1	Coil 2	Coil 3	Coil 4
Coil 1	450 mH	70.83 mH	68.71 mH	70.77 mH
Coil 2	70.83 mH	451.27 mH	70.80 mH	68.85 mH
Coil 3	68.71 mH	70.80 mH	450.65 mH	70.75 mH
Coil 4	70.77 mH	68.85 mH	70.751 mH	450.91 mH

### III. MATHEMATICAL MODEL OF QELPS

#### A Single Coil Model of QELPS

A single coil analysis will be approximated as the same as the other coils in the system to produce the mathematical equation for the calculation of the model's equivalent Reluctance. This study is carried out on the assumption that all coils are uniform in size and spaced at equal intervals. The coil and bar parameters are shown in Figure 5. Where  $t$  is the thickness of the coil,  $w_c$  is the width of the coil,  $l_c$  is the length of the coil,  $l_g$  is the airgap length between the coil and bar,  $h_b$  is the height of the bar.

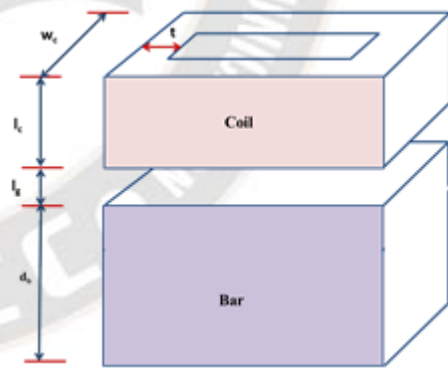


Figure 5. Single coil model of QELPS

For finding the number of flux paths and how the flux moves through the system FEMM freeware is used. After the building the 2D model of QELPS in FEMM, the flux lines are observed and represented in Figure 6. These flux lines are used to identify and calculate the reluctance of the overall system. Due to current flow, flux is emanating from the electromagnetic coil. An expression for permeance is derived using the flux volume and the flux flow's mean length. The flux is moving through the system's coil, airgap, and bar. Each flow path's mean length and permeance are expressed after the volume.

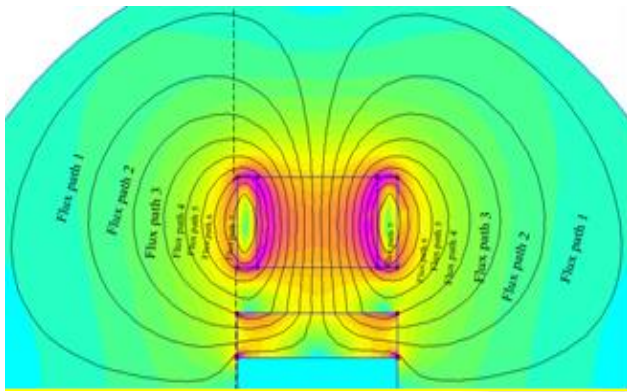


Figure 6. Identification of flux paths

Flux from the Electromagnetic coil in Flux path 1:

$$\text{Volume of the flux tube} = \left(\frac{h_c-t}{5}\right) l_c w_c \quad (6)$$

$$\text{Mean length of the flux line} = l_c \quad (7)$$

$$\text{Permeance} = \frac{\mu_0 \mu_r (h_c-t) w_c}{5 l_c} \quad (8)$$

Flux in the airgap in Flux path 1:

$$\text{Volume of the flux tube} = \frac{1}{2} \left[ \frac{4h_c+5l_p-9t}{20} \right] l_g w_p \quad (9)$$

$$\text{Mean length of the flux line} = l_g \quad (10)$$

$$\text{Permeance} = \frac{\mu_0 (4h_c+5l_p-9t) w_p}{40 l_g} \quad (11)$$

Flux in the bar in Flux path 1:

$$\text{Volume of the flux tube} = \pi \frac{d_b}{3} \left( \frac{3l_p+t}{4} \right) w_p \quad (12)$$

$$\text{Mean length} = \frac{\pi}{2} \sqrt{\frac{(7l_p+t)^2}{8} + \left(\frac{5d_b}{8}\right)^2} \quad (13)$$

$$\text{Permeance} = \frac{2\mu_0 \mu_r d_b w_p}{\pi} \left[ \frac{2l_p}{\sqrt{l_p^2 + \frac{d_b^2}{4}}} - \frac{1}{\sqrt{\frac{(7l_p+t)^2}{5} + \left(\frac{5d_b}{12}\right)^2}} \right] \quad (14)$$

Using Eq.(8), (11) & (14), equivalent reluctance of one flux path is derived. In the similar pattern, equivalent reluctance is derived for the remaining flux paths.

#### IV. IMPLEMENTATION OF QELPS FOR LINEAR MOTION TRACK

Modern robotics is dealing with ever-increasing demands for flexible automation. One example is linear tracks to increase the robot's workspace. The linear track's flaws reduce precision, contrasting with the precise robot systems required for current

applications [24]. Identification of the non-linearities of the linear path is necessary to improve the accuracy of the system consisting of robots and a linear track.

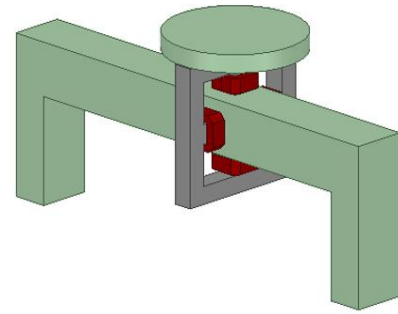


Figure 7. 3D model of QELPS

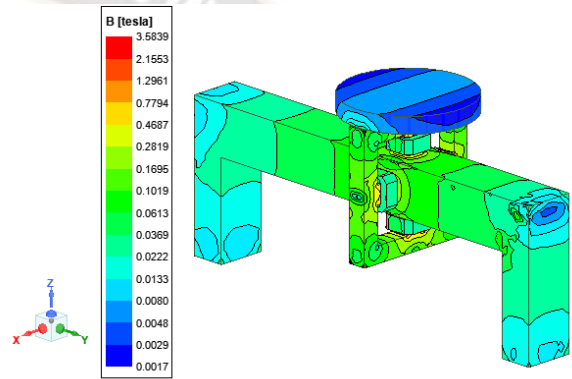


Figure 8. Magnetic density in QELPS

This paper presents a design of QELPS for the exact integration of track movements. Figure 7 illustrates the 3D model of the QELPS-based linear motion track. On the top of the yoke, a non-conducting plate is placed. The conducting plate will be the utility place. The length of the sliding bar is a variable, which varies based on the operation area in the industry. For testing purposes, a current of 1000A is injected into the coils. Complete model magnetic behavior is presented in Figure 8, Figure 9, and Figure 10. In the 3D FEM analysis, the maximum flux density of 3.5839 Tesla is observed in the pole shoes of the yoke, and maximum intensity of  $1.168 \times 10^5$  A/m and maximum current density of  $7.9826 \times 10^6$  A/m<sup>2</sup> are observed in the coils of the system as shown in Figure 10.

#### V. INTERACTIVE QELPS DESIGN ALGORITHM IMPLEMENTATION

Based on this analysis it is clearing the possibilities of implementing the QELPS as a linear drive system. An interactive design algorithm is much needed to design various ranges of QELPS. The main objective is to develop QELPS as per the user requirements.

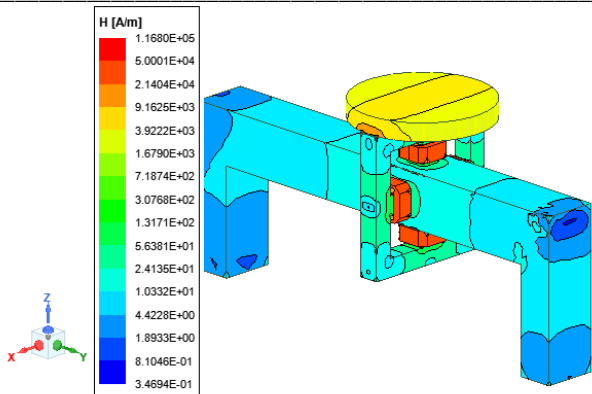


Figure 9. Magnetic intensity in QELPS

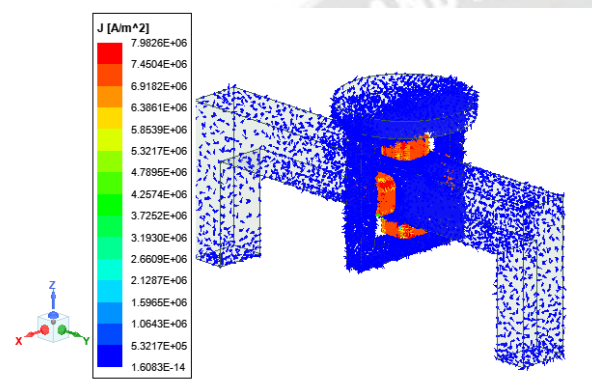


Figure 10. Current Density in QELPS

The basic information the user must provide is track parameters such as length, side length, and side width. The final output of this algorithm will be the dimension of QELPS mentioned in Table II. Such as the length of the coil, the side length of the coil, the side width of the coil, the number of turns, the number of layers in the coil, and the outer yoke dimensions.

TABLE 2: QELPS DESIGN VALUES FROM DESIGN ALGORITHM

Parameters	Values
Number of turns for each layer	22.00
Number of turns for each coil	242
Number of layers for each coil	11
Height of coil for each coil	0.043 m
Thickness of the coil	0.0092 m
Number of poles	4
Velocity obtained	4.90 m/sec

- Step 1: Start the program by inputting basic parameters such as the absolute and relative permeability, as well as the absolute and relative permittivity of the materials.
- Step 2: Prompt the user to enter the length, width, height of the track, and required velocity of operation.
- Step 3: Initialize the number of turns and layers to the starting point, which is 1.

Step 4: Calculate inductance values, mutual inductance values, force values, and velocities for each turn.

Step 5: Check if the user's required velocity is close to the calculated value. If it matches, the program will terminate. Otherwise, return to Step 3, increment the number of turns, and recalculate the values.

Step 6: Display the final output parameters, including the number of layers, coil height, coil length, coil width, coil thickness, and the obtained force.

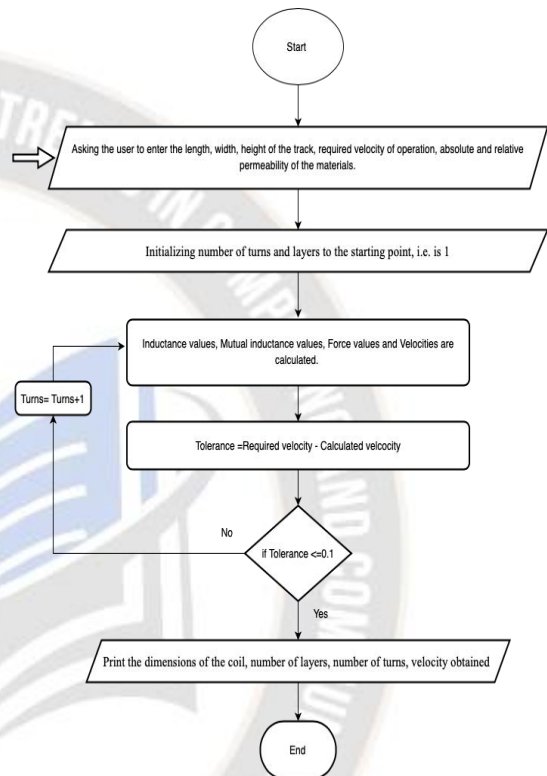


Figure 11. QELPS Flowchart

## VI. RESULTS AND DISCUSSIONS

In Figure 12, the power circuit of the QELPS is presented. The power circuit of QELPS is simulated in ANSYS Simplorer. The model of QELPS is developed using the ANSYS Twin builder. Using Maxwell 3D, the 3D model of QELPS is designed and linked with the Simplorer using Twin Builder. Twin Builder produces an equivalent circuit according to the simulation analysis in Maxwell.

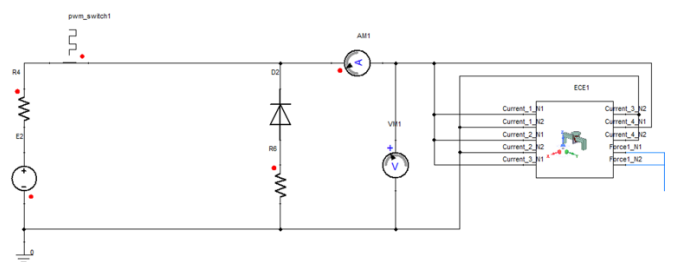


Figure 12. Power circuit diagram of QELPS

Current and position are the input variables, and force is the output variable, the source with an initial voltage of 30V. The resistance values in the circuit are R4 of 0.001  $\Omega$  and R6 of 0.2  $\Omega$ . For testing purposes, the PWM switch is considered as the switching device. The PWM switch with a time period of 20 msec, a duty cycle of 0.5, and an Initial delay of 1 msec. As illustrated in Figure 13, the output force terminal is linked to the translational mass block representing displacement force and the translational limit stop block represents displacement force for a more practical approach. The armature's bar mass is 1000 grams, and the damping coefficient is 100000 Ns/m, with upper and lower position limits of 0.05 m and 0.01 m, respectively. The force output is connected to the translational mass and friction, to understand the working of the system. A damping coefficient of  $10 \times 10^5$  Ns/m and a spring rate of  $10 \times 10^5$  N/m are considered in the translation friction model.

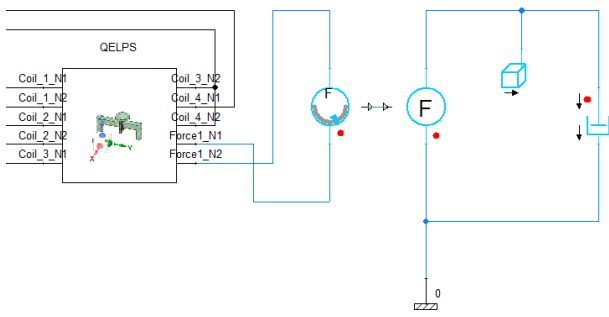


Figure 13. Mechanical translational circuit diagram of QELPS

In Figure 13, the mechanical translational circuit diagram of QELPS is presented. In which a force meter is used to measure the Lorentz force produced from the coils over projectile and corresponding mass and damping were presented in the ANSYS Simplorer circuit.

After execution, the square-shaped yoke's force, current, velocity and acceleration are presented in Figure 14, Figure 15, Figure 16, and Figure 17.

return to the baseline. This cycle of switching the PWM switch on and off continues to allow the smooth linear position movement of the QELPS. This is a preliminary study on implementing QELPS for linear motion track.

Figure 15 illustrates the current in QELPS. Time is plotted on the x-axis in milliseconds, and the current, measured in amperes, is plotted on the y-axis. When the PWM switch is turned on, there is an initial delay of 1 millisecond, after which the current transiently increases to 580 amperes based on the pulse width. As the switch turns off, the current decreases to zero amperes. The cycle of alternately switching the PWM switch on and off continues. The current direction can be reversed for both the forward and reverse operation of the circuit. Additionally, adding resistance and a diode to the circuit can limit the reverse current.

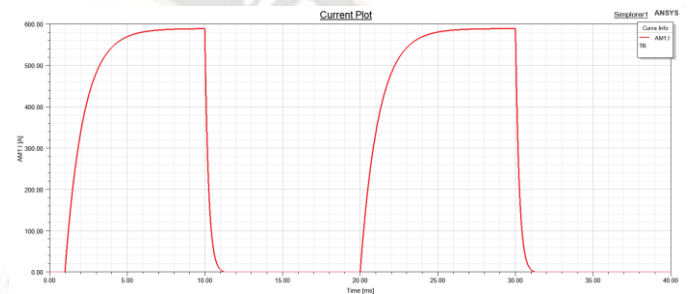


Figure 15. Current Profile of QELPS

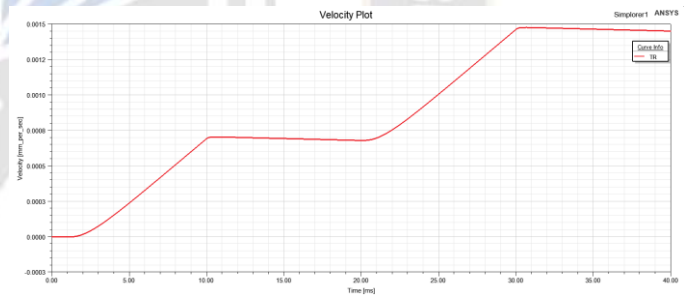


Figure 16. Velocity of QELPS

In Figure 16, time is plotted on the x-axis in milliseconds, and velocity measured in millimeters per second is plotted on the y-axis. When the PWM switch is turned on, the velocity ramps up to 0.00074 mm/s. When the switch is turned off in the second half cycle, the velocity continues at the same speed. Later, when the switch is turned on in the second cycle, the velocity increases from the preexisting speed to 0.0014 mm/s. After that, it remains constant for the second half of the cycle. Figure 17 depicts the acceleration of QELPS. Time is plotted on the x-axis in msec and acceleration measured in  $\text{mm}/\text{sec}^2$  is plotted on the Y-axis. Like the force generated, when the PWM switch is turned on the acceleration of the mass also begins to increase after an initial delay of 1msec to 0.09  $\text{mm}/\text{sec}$ .

Later in the second half of the cycle when the switch is turned off the acceleration also reduces to the baseline. This is a

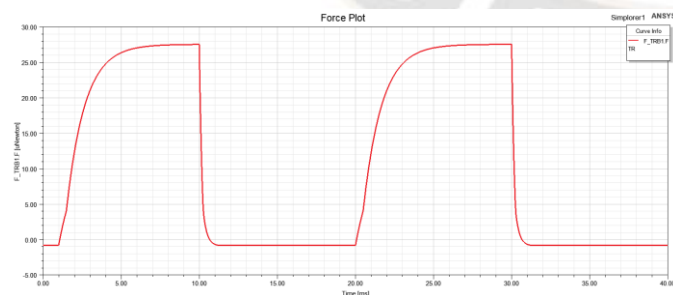


Figure 14. Force Profile of QELPS

The force profile of the QELPS is presented in Figure 14 for two cycles. When the PWM switch is turned on, after an initial delay of 1 millisecond, the Lorentz force increases to 27.6 newtons based on the pulse width i.e., based on the requirement of operation. Switching off the PWM switch causes the force to

preliminary study on the implementation of QELPS for linear motion track. Using QELPS for linear motion track is its simple control operation. The circuit's current is the main parameter on which the whole process depends. More sophisticated research is needed to implement QELPS for linear track applications.

understanding, encouragement, and unwavering belief in my abilities.

### CONFLICTS OF INTEREST

The authors do not have any conflicts of interest to declare concerning this research work.

### REFERENCES

- [1] Laithwaite ER, Nasar SA. "Linear-motion electrical machines," Proceedings of the IEEE. 1970,58(4),531–542. <https://doi.org/10.1109/PROC.1970.7692>.
- [2] Cassat A, Corsi N, Moser R, Wavre N. "Direct linear drives: Market and performance status," In Proceedings of the 4th International Symposium on Linear Drives for Industry Applications 2003 Sep 8 (pp. 1-11). UK: Birmingham.
- [3] Boldea I, Naser SA. Linear motion electromagnetic systems. (First). Wiley-Interscience Hardcover, Fair, United kingdom.1985.
- [4] Kim SW, Jung HK, Hahn SY. "Optimal design of multistage coilgun," IEEE transactions on magnetics. 1996 Mar, 32(2), 505-8. <https://doi.org/10.1109/20.486539>.
- [5] Cupertino F, Naso D, Mininno E, Turchiano B. "Sliding-mode control with double boundary layer for robust compensation of payload mass and friction in linear motors," IEEE Transactions on Industry Applications. 2009 Jul 14;45(5):1688-96. <https://doi.org/10.1109/TIA.2009.2027521>
- [6] Ferkova Z, Franko M, Kuchta J, Rafajdus P. "Electromagnetic design of ironless permanent magnet synchronous linear motor," In 2008 International Symposium on Power Electronics, Electrical Drives, Automation and Motion 2008 Jun 11 (pp. 721-726). <https://doi.org/10.1109/SPEEDHAM.2008.4581085>
- [7] Lesquesne B. "Permanent magnet linear motors for short strokes", Conference Record of the 1992 IEEE Industry Applications Society Annual Meeting. 1992,162–170. <https://doi.org/10.1109/IAS.1992.244449>.
- [8] Zhu Y, Wang Y, Yan Z, Dong L, Xie X, Li H. "Multipole Field Electromagnetic Launcher," IEEE Transactions on Magnetics. 2010, 46(7), 2622–2627. <https://doi.org/10.1109/TMAG.2010.2044416>.
- [9] Xue X, Shu T, Yang Z, Feng G. "A New Electromagnetic Launcher by Sextupole Rails: Electromagnetic Propulsion and Shielding Numerical Validation," IEEE Transactions on Plasma Science. 2017, 45(9), 2541–2545. <https://doi.org/10.1109/TPS.2017.2728688>.
- [10] Luo W, Wang Y, Gui Z, Yan Z, Chen W. "Connection pattern research and experimental realization of single-stage multipole field electromagnetic launcher," IEEE Transactions on Plasma Science. 2013, 41(11), 3173–3179. <https://doi.org/10.1109/TPS.2013.2281240>.
- [11] Musolino A, Rizzo R, Tripodi E. "Travelling wave multi-pole field electromagnetic launcher: An SOVP analytical model," IEEE Transactions on Plasma Science. 2013, 41(5), 1201–1208. <https://doi.org/10.1109/TPS.2013.2246839>.
- [12] Zhu Y, Wang Y, Chen W, Yan Z, Li H. "Analysis and evaluation of three-stage twisty octapole field electromagnetic launcher,"

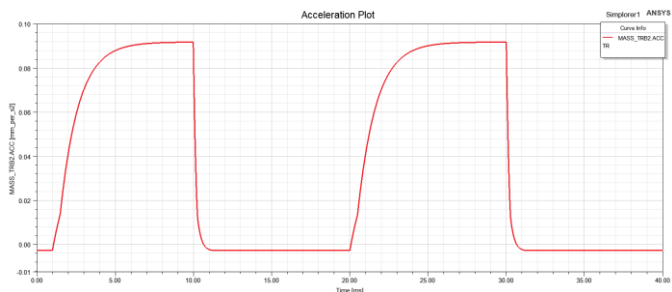


Figure 17. Acceleration of QELPS

### VII. SUMMARY AND CONCLUSION

The article delves into the technical aspects of the design algorithm and modeling process of a Quadrupole Electromagnetic linear position system (QELPS) utilized in linear motion tracking applications within the manufacturing industries. The QELPS functions as a non-contact sensor capable of accurately measuring the position and velocity of a moving object. The article provides a comprehensive account of the design algorithm for the QELPS, encompassing the selection of magnetic materials, calculation of magnetic field strength, and determination of the optimal sensor position.

Additionally, the article explores the modeling of the QELPS, including implementing finite element analysis (FEA) to simulate the magnetic field and utilising ANSYS for data analysis. This article thoroughly explains the underlying theory behind the QELPS, including the principles governing magnetic fields and the quadrupole configuration. Integrating QELPS within manufacturing industries can yield numerous advantages, such as precise control over object positioning throughout the manufacturing process and the ability to detect deviations from the intended path. These benefits can contribute to enhanced product quality and waste reduction. The QELPS exhibits promise in linear motion applications based on the obtained values, and further expansion of its implementation to various domains can be facilitated through optimal design and the incorporation of a suitable power circuit.

### ACKNOWLEDGMENT

The research was carried out at a Research lab in the Department of Electrical, Electronics, and Communication Engineering, GITAM School of Technology, GITAM deemed to be University, in Visakhapatnam. I sincerely acknowledge my Research supervisor, Dr Kondamudi Srichandan for his invaluable guidance, unwavering support, and expertise throughout this research. I thank my family and friends for their



- IEEE Transactions on Plasma Science. 2012, 40(5 PART 2), 1399–1406. <https://doi.org/10.1109/TPS.2012.2188530>.
- [13] Engel TG, Veracka MJ. “The voltage–current scaling relationship and impedance of DC electromagnetic launchers,” IEEE Transactions on Plasma Science. 2015 Apr 9;43(5):1271-76. <https://doi.org/10.1109/TPS.2015.2418053>
- [14] Gutierrez H, Meinke R, Fernando T, Kirk D. “Non-contact DC electromagnetic propulsion by multipole transversal field: Numerical and experimental validation,” IEEE Transactions on Magnetics. 2016 Apr 13;52(8):1-0. <https://doi.org/10.1109/TMAG.2016.2553644>
- [15] Kondamudi SC, Thotakura S, Rao Pasumarthi M, Ramakrishna Reddy G, Sathyaraj SM, Jiang XX. “A novel type coil-multipole field hybrid electromagnetic launching system,” Results in Physics. 2019,15,102786. <https://doi.org/10.1016/j.rinp.2019.102786>.
- [16] Kondamudi S, Pasumarthi MR. “Computations of magnetic forces in Multipole Field Electromagnetic Launcher,” International Journal of Mathematical, Engineering and Management Sciences. 2019,4(3),761–774. <https://doi.org/10.33889/IJMEMS.2019.4.3-059>.
- [17] Meinke RB, Goodzeit CL, Ball MJ. “Modulated double-helix quadrupole magnets,” IEEE Transactions on Applied Superconductivity. 2003, 13(2), 1369–1372. <https://doi.org/10.1109/TASC.2003.812674>.
- [18] Thotakura S, Srichandan K, Mallikarjuna Rao P. “A Novel Configuration of Multi-stage Outrunner Electromagnetic Launching for Aircraft Catapult System,” 2020:364–372. [https://doi.org/10.1007/978-3-030-24318-0\\_44](https://doi.org/10.1007/978-3-030-24318-0_44).
- [19] Yang Z, Feng G, Xue X, Shu T. “An Electromagnetic Rail Launcher by Quadrupole Magnetic Field for Heavy Intelligent Projectiles,” IEEE Transactions on Plasma Science. 2017, 45(7), 1095–1100. <https://doi.org/10.1109/TPS.2016.2646377>.
- [20] Zabar Z, Naot Y, Birenbaum L, Levi E, Joshi PN. “Design and Power Conditioning for the Coil-Gun,” IEEE Transactions on Magnetics. 1989, 25(1), 627–631. <https://doi.org/10.1109/20.22613>.
- [21] Dong L, Sun S, Wu H. “Study of capacitor parameters on the optimal trigger position of multipole field reconnection electromagnetic launcher,” IEEE Transactions on Plasma Science. 2021 Jun 9;49(7):2153-60. <https://doi.org/10.1109/TPS.2021.3084632>
- [22] Manohar K, Srichandan K. Design “Optimization of Quad-pole Electromagnetic Ejection Device using Particle Swarm Optimization. Proceedings,” 2021 IEEE International Conference on Intelligent Systems, Smart and Green Technologies, ICISSTG 2021., 2021, 52–56. <https://doi.org/10.1109/ICISSTG52025.2021.00022>.
- [23] Manohar K, Srichandan K. “Analysis of Quadrupole Magnetic Field Reluctance-Based Launcher With Different Coil Switching Patterns,” IEEE Transactions on Plasma Science. 2023, 51(5), 1370-1376, <https://doi.org/10.1109/TPS.2023.3266515>.
- [24] Kleinkes, M., Neddermeyer, W., & Schnell, M. “Improved method for highly accurate integration of track motions,” ICINCO 2006 - 3rd International Conference on Informatics in Control, Automation and Robotics. Proceedings, RA, 2006, 469–473. <https://doi.org/10.5220/0001203504690473>
- [25] Yan Z, Long X, Lu F, Wang Y, Liu H. “Study of Single-Stage Double-Armature Multipole Field Electromagnetic Launcher,” IEEE Transactions on Plasma Science. 2017, 45(8), 2381–2386. <https://doi.org/10.1109/TPS.2017.2716421>.
- [26] Shokair IR. “Projectile Transverse Motion and Stability in Electromagnetic Induction Launchers,” IEEE Transactions on Magnetics. 1995, 31(1), 504–509. <https://doi.org/10.1109/20.364641>.
- [27] Gordon S, Hillery MT. “Development of a high-speed CNC cutting machine using linear motors,”. Journal of Materials Processing Technology. 2005 Aug 20;166(3):321-329. <https://doi.org/10.1016/j.jmatprotec.2003.08.009>
- [28] Prasad G, Srichandan K. “Performance Evaluation on Two Wing Ring Type Armature with Inductive Type Electromagnetic Launching System,” In 2022 IEEE 10th Power India International Conference (PIICON) 2022 Nov 25 (pp. 1-5). IEEE. <https://doi.org/10.1109/PIICON56320.2022.10045133>.